Asian J. of Adv. Basic Sci.: 2(1), 61-69
ISSN (Online): 2347 - 4114
www.ajabs.org

Synthesis and Optical characterization of Gadolinium Praseodymium Oxalate, Gadolinium Dysprosium Oxalate, and Dysprosium Praseodymium Oxalate crystals

V. Thomas[*], A. Elizabeth[**], C. Joseph[***], P. R. Biju[****] and G. Jose[*****] and N. V. Unnikrishnan[******]
[*] *Department of Physics, SB College, Changanachery, INDIA*
Email ID: vinoythoma@gmail.com
[**], [***] & [****] *School of Pure and Applied Physics, Mahatma Gandhi University, Kottayam, INDIA -686560*
[*****] *Department of Physics, Christian College -689122, University of Kerala, INDIA -689122*

(Received 03 Jan, 2014, Accepted 01 Feb, 2014)

ABSTRACT: Preparation and optical characterization of dysprosium gadolinium oxalate (DGO), dysprosium praseodymium oxalate (DPO) and gadolinium praseodymium oxalate (GPO) single crystals are reported. The crystals were grown using silica gel technique, by the controlled reaction of rare earth nitrates with oxalic acid. Crystals were characterized using X-ray powder diffraction and optical absorption studies. Radiative transition probability, fluorescence branching ratio and radiative lifetime of Dy^{3+} and Pr^{3+}in the crystals are evaluated by the parameterization of the absorption spectrum using Judd-Ofelt theory.

Keywords: oxalate crystals, rare earths, X-ray diffraction, and Judd-Ofelt theory.

INTRODUCTION

Compact and efficient all solid state lasers emitting in the visible spectral region are of great interest for a number of applications in medicine, biology, metrology, optical storage and display technology. It is well known that rare earth ions have number of efficient and narrow emission lines in the visible and NIR wavelength region. Optical absorption and emission properties of rare earth ions in transparent crystals, glasses, ceramics and polymers are widely investigated for potential applications in these wavelength regions [(1-5)]. The optical properties of rare earth ions Ce^{3+}, Sm^{3+}, Eu^{3+}, Er^{3+},Tb^{3+}, Yb^{3+}, Pr^{3+}, $Nd^{3+}$and Dy^{3+}[(6-14)] incorporated into crystals have been reported. Of the various rare earth crystals, rare earth oxalates are of particular importance due to their wide applicability in the fields of molecular based magnetic materials, luminescent materials and precursor for superconducting oxides. The coordinating ability of the oxalate ligand makes it superior among the rare earth compounds and also the subject of experimental and theoretical studies [(15-17)]. Theconcentration of rare earth ions in these crystals can be of the order of 10^{21} ions/cm^3, which encourages a high optical gain of the material. Single crystals of rare earth oxalates such as cerium oxalate, holmium oxalate and gadolinium samarium oxalate etc. have been synthesized and studied in recent years [(18-21)].However synthesis and detailed spectroscopic studies of rare earth oxalates DPO, GPO and DGO were rarely done. The present authors made an attempt to obtain the spectroscopic parameters of Dy^{3+} in mixed oxalate crystals [(22-23)]. To fabricate in optical devices, detailed information of all rare earth ions in the crystal is essential. The crystals DPO, GPO and DGO are expected to have potential applications because of the relatively high quantum efficiency of their radiative transitions. Hence synthesis and detailed investigation of these mixed rare earth oxalate crystals deserves special attention and importance.

MATERIAL AND METHODS

Single crystals of GPO,GDO and DPO were grown by the hydro silica gel method []ref, The growth was accomplished by the controlled diffusion of rare earth ions (Gd, Dy and Pr) through silica gel

impregnated with oxalic acid. For the preparation of the gel, sodium meta silicate solution of desired specific gravity was mixed with 1M oxalic acid. An aqueous mixture of equal volume of nitrates of rare earths (99.99% purity, Sigma Aldrich) acidified with concentrated nitric acid was poured over the set gel. The diffusion of outer electrolyte into the gel promotes the reaction of rare earths with oxalate ions, which results in the crystallization of double oxalate crystals containing Gd^{3+}, Dy^{3+} and Pr^{3+} ions. A representative equation for the reaction can be written as

$$X(NO_3)_3.nH_2O + Y(NO_3)_3.nH_2O + 3H_2C_2O_4 \rightarrow XY(C_2O_4)_3.nH_2O + 6HNO_3$$

Here X and Y represents the rare earths. A gel density of 1.04 gm/cc and pH6 favors growth of well-shaped good quality crystals (Figure 1). Optical spectra of the crystals were recorded with UV-Visible spectrophotometer (Shimadzu UVPC 2401). All the experiments were done at room temperature. X-ray diffraction pattern of the grown samples of crystals was recorded on a Philips model PW 1710 diffractometry with nickel filtered CuKα radiation

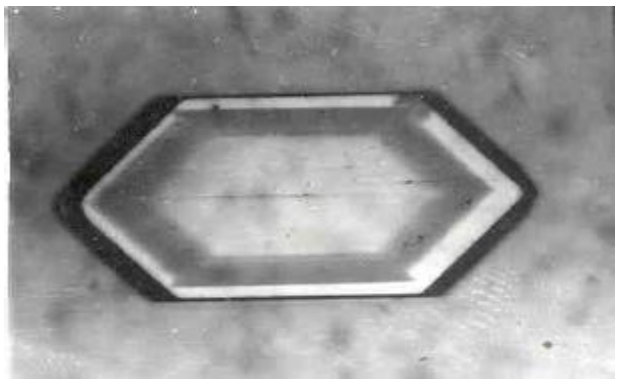

Figure 1: Typical photograph of the mixed oxalate (DGO) crystal.

RESULTS AND DISCUSSION

1. Structural studies:

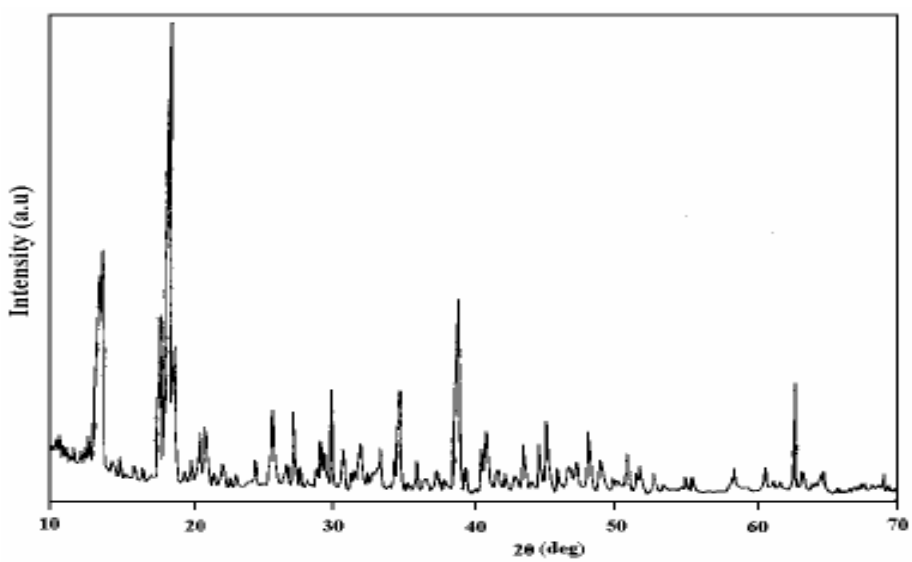

Figure 2: X-ray diffraction pattern of rare earth oxalate crystal (DGO)

Figure 2 shows a representative X-ray diffraction pattern of the crystal in the 2θ range 10^0-70^0. The well-defined diffraction peaks establishes the crystalline nature of the sample. The ionic radii of gadolinium,

praseodymium and dysprosium are comparable, and hence identical crystal structure for these mixed crystals can be expected [21].All the lattice parameters of crystals are given in Table 1. The d-values of the crystals are found to be comparable with that of single oxalates [18]. The diffraction peaks were indexed assuming that all the crystals crystallize in the monoclinic system with space group $P2_{1/c}$. The narrow deviation of the lattice parameters of these crystals with that of other oxalate crystals confirms the assumption that the oxalate crystals containing two rare earths of comparable ionic radii can be formed by substitutional exchange of ions and are iso-structural with single oxalate crystals.

Table 1: Lattice parameters of crystals.

	GDO	GPO	DPO
Chemical formula	$DyGd(C_2O_4)_3.10H_2O$	$PrGd(C_2O_4)_3.10H_2O$	$DyPr(C_2O_4)_3.10H_2O$
Space group	$P2_{1/c}$	$P2_{1/c}$	$P2_{1/c}$
a (A^0)	10.985	11.099	11.02
b(A^0)	9.598	9.617	9.603
c (A^0)	9.977	10.15	9.99
β	114.14^0	114.28^0	114.18^0
Volume ($A^0)^3$	959.92	987.67	965.4

2. Optical absorption studies: Optical absorption spectra of the crystals were recorded with UV-visible Spectrophotometer (Shimadzu-UVPC 2401) at room temperature The electronic transitions of the trivalent lanthanides can be electric dipole, magnetic dipole or electric quadrupole in nature [24]. For Dy^{3+} ion all the transitions occur from $^6H_{15/2}$ ground state and for Pr^{3+} all the transitions occur from the $^3H_4$ ground state. The strong absorption peak at around 250nm is assigned to that of the oxalate group and the absorption peaks in the 280-310nm range are related to the transitions of Gd^{3+}ions $^8S_{7/2} \rightarrow {}^6D_J$, J=9/2,5/2,7/2,1/2).

3. Oscillator strengths: Intensities of all the absorption bands are evaluated by measuring their oscillator strengths (f), which are found to be proportional to the area under the absorption line shapes. For single peaks such as $^1D_2$ the absorption band was integrated directly after subtracting the background loss. To resolve the overlapping absorption bands such as $^3P_2$, $^3P_1$ etc., a Gaussian fit was performed to each peak in order to determine the peak position and the area was determined using Simpson's rule for numerical integration. The calculated areas were then scaled to match the total area of the overlapping bands. The experimental values of the oscillator strengths is expressed in terms of molar extinction coefficient (ε) and the energy of the transition in wave numbers (ν) by the expression [25].

$$f = 4.32 \times 10^{-9} \int \varepsilon(\nu) d\nu \qquad \text{---------- (1)}$$

Where dν is the band width at half height and (ε) is the molar extinction coefficient at a given energyν.

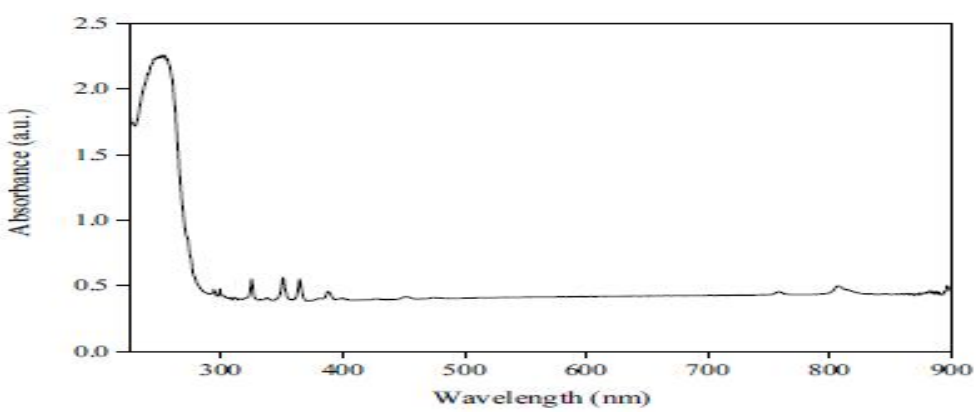

Figure 3: Representative absorption spectra of the prepared crystal (DGO).

4. Judd-Ofelt Analysis: According to Judd-Ofelt [26, 27] (JO) theory oscillator strengths of an intraconfigurational electric dipole transition within the 4f shell of a trivalent rare earth ion can be obtained from the relationship.

$$f = \frac{8\pi^2 mc\nu}{(2J+1)3h}\frac{(n^2+2)^2}{9n}\sum_{\lambda=2,4,6}\Omega_\lambda(\langle f^N[\alpha SL]J\|U^\lambda\|f^N[\alpha'S'L']J'\rangle) \qquad \text{-------- (2)}$$

Where the three terms $(\langle f^N[\alpha SL]J\|U^\lambda\|f^N[\alpha'S'L']J'\rangle)$ are the doubly reduced unit tensor operators calculated in the intermediate coupling approximations Ω_λ, the Judd-Ofelt intensity parameters, ν the mean energy of the transition. (2J+1) is the ground state degeneracy and n the refractive index of the medium. Using the matrix elements (U^λ) given in the literature [28] and the experimental oscillator strengths (f_{mes}), the intensity parameters (Ω_λ) have been evaluated by least square programming. To obtain reliable JO parameters a sufficient number of ground state transitions must be used. In practice at least five or six are taken. Here Gd^{3+} has only two transitions and it is not possible to calculate JO parameters of Gd^{3+} in the present crystal matrices [28]. Using the JO theory, the electric dipole line strengths S_{ed} can be found using the expression.

$$S_{ed}(aJ,bJ) = e^2\sum_{\lambda=2,4,6}\Omega_\lambda(\langle f^N[\alpha SL]J\|U^\lambda\|f^N[\alpha'S'L']J'\rangle) \qquad \text{---------- (3)}$$

The squared reduced matrix elements $\|U^\lambda\|^2$ are calculated in the intermediate coupling case. As the variations in these squared reduced matrix elements are negligible from host to host, we have used the parameters given by *Carnall et al* [28]. The experimental and calculated oscillator strengths and electric dipole line strengths of the observed transitions are presented in Tables 2 and 3. The experimentally obtained oscillator strengths of various absorption transitions of Dy^{3+} and Pr^{3+} ions in the crystal matrices are found to be in good agreement with that of other crystal matrices. An examination of these oscillator strengths clearly shows that the oscillator strengths of the $^3H_4 \rightarrow {}^3P_2$ transition is extremely large in comparison with all other transitions. These hypersensitive transitions are observed in many rare earth ions also show anomalous nature irrespective of the matrix environments. This hypersensitive transitions satisfy the selection rule $\Delta S = 0$, $\Delta J = \pm 2$. Because of the anomalous nature of this transition it is usually excluded from the calculation of the JO parameters. The calculated values of the JO parameters are given in Table 4. A close observation of the absorption transition matrix elements of Pr^{3+} ion shows that the value of Ω_2 parameters entirely depends on the $^3H_4 \rightarrow {}^3F_2$ transition because of the high value of $\langle {}^3H_4\|U^2\|{}^3F_2\rangle$. Even though this matrix element is comparatively larger, the oscillator strength of the transition is comparable to all other transitions except the hypersensitive transition $^3H_4 \rightarrow {}^3P_2$ transition. Therefore the value of Ω_2 entirely depends on the nature of the $^3H_4 \rightarrow {}^3F_2$ transition. If this transition is excluded in the calculation, the value of Ω_2 will be extremely small in comparison with Ω_4 or Ω_6 and in some cases it assumes a negative value [29, 30].

Table 2: Oscillator strengths and electric dipole line strengths of all the observed transitions of Dy^{3+} in GDO and DPO crystals.

	DGO		DPO	
Transitions from $^6H_{15/2}$	**$f_{mes}(10^{-6})$**	**$S_{ed}(10^{-20}cm^2)$**	**$f_{mes}(10^{-6})$**	**$S_{ed}(10^{-20}cm^2)$**
$^4H_{11/2}$	0.3326	0.036	-	-
$^6P_{3/2}$	1.598	0.685	2.67	0.10
$^4I_{9/2}$	0.2592	0.0024	0.44	0.01

$^6P_{7/2}$	2.89	1.12	4.40	0.19
$^6P_{5/2}$	2.445	0.436	3.59	0.16
$^4F_{7/2}$	1.041	0.3189	1.71	0.08
$^4G_{11/2}$	0.1339	0.0733		
$^4I_{15/2}$	0.589	0.467	0.38	0.02
$^6F_{3/2}$	0.447	0.385	1.01	0.09
$^6F_{5/2}$	3.047	2.27	4.89	0.40
$^6F_{7/2}$	0.112	4.26	-	-
$^6H_{5/2}$	0.596	0.016	-	-

Table 3: Oscillator strengths and electric dipole line strengths of all the observed transitions of Pr^{3+} in DPO and GPO crystals.

	GPO		DPO	
Transitionsfrom $^3H_4$	**$f_{mes}(10^{-6})$**	**$S_{ed}(10^{-20}cm^2)$**	**$f_{mes}(10^{-6})$**	**$S_{ed}(10^{-20}cm^2)$**
$^3P_2$	18.94	0.58	13.38	0.58
$^3P_1$	8.89	0.25	5.38	0.25
$^3P_0$	3.96	0.13	2.42	0.13
$^1D_2$	12.35	0.47	7.43	0.47

Table 4: Judd-Ofelt (JO) parameters of Dy^{3+} and Pr^{3+} ions in the crystals.

	Dy^{3+} ions in		Pr^{3+} ions in	
	GDO	**DPO**	**GPO**	**DPO**
Ω_2 (10^{-20} cm^2)	6.31	15.22	2.86	6.15
Ω_4 (10^{-20} cm^2)	2.05	1.15	1.08	0.73
Ω_6 (10^{-20} cm^2)	6.26	2.75	3.99	2.83

5. Radiative parameters: The present crystalline matrix contains trivalent Dy and Pr as the luminescent centers. Hence the luminescent properties of both the ions contribute to the total radiative nature of the crystal as a whole. By exploiting the JO theory the transition intensities and radiative properties of Dy^{3+} and Pr^{3+} ions in these crystals are predicted. The radiative parameters like radiative transition probability (A), radiative life time (τrad), fluorescence branching ratio (β) are evaluated using the expressions

$$A[(S,L,J):(S',L',J')] = \frac{64\pi^4 n\nu^3 (n^2+2)^2}{3h(2J+1)} S_{ed} \qquad \text{---------- (4)}$$

$$\beta = \frac{A[(S,L,J):(S',L',J')]}{\sum A[(S,L,J):(S',L',J')]} \qquad \text{---------- (5)}$$

$$\tau_{rad} = \frac{1}{\sum A[(S,L,J):(S',L',J')]} \qquad \text{---------- (6)}$$

The integrated absorption crossection (σ_a) for stimulated emission is evaluated using the Fuchtbauer-Ladenberg equation [25].

$$\sigma_a = \frac{1}{\nu^2}\frac{A}{8\pi c n^2} \qquad \text{---------- (7)}$$

Where ν is the energy of the transition, c is the velocity of light and n is the refractive index of the medium. The calculated radiative parameters of Dy^{3+} and Pr^{3+} in GDO,GPO and DPO are summarised in Tables 5 and 6.

For Dy^{3+} ion the meta stable state $^4F_{9/2}$ can be connected with the lower states via, $^4F_{9/2}\rightarrow{}^6F_{1/2}$, $^6F_{3/2}$, $^6F_{5/2}$, $^6F_{7/2}$, $^6H_{5/2}$, $^6H_{7/2}$, $^6F_{9/2}$, $^6H_{11/2}$, $^6H_{13/2}$, $^6H_{15/2}$. All these transitions can be assumed to be electric dipole in nature. The electric dipole oscillator strengths (S_{ed}) and transition probabilities (A) are found to be a linear combination of Ω_2, Ω_4 and Ω_6. For Dy^{3+} the JO parameters show a tendency $\Omega_2 > \Omega_6 > \Omega_4$. These parameters are found to vary from site to site. The Ω_2 parameter involves the longer range terms in the crystal field potential and is the most sensitive to the local structural changes. The branching ratios and the transition probabilities are found to be maximum for the $^4F_{9/2} \rightarrow {}^6H_{13/2}$ transition. For a large stimulated emission cross section one wants the branching ratio (□) to be as large as possible.

For Pr^{3+} ion the meta stable state for laser transition is $^1D_2$. In this case also the S_{ed}, and transition probabilities are found to be a linear combination of Ω_2, Ω_4 and Ω_6 parameters. The JO parameters show a tendency $\Omega_6 > \Omega_2 > \Omega_4$ in GPO crystal and $\Omega_2 > \Omega_6 > \Omega_4$ in DPO crystal. The branching ratio and transition probabilities are found to be maximum for the $^1D_2 \rightarrow {}^3H_4$ transition.

Table 5: Calculated radiative parameters of Pr^{3+} ion in the DPO crystal.

		GPO						DPO					
Transition from $^1D_2$	**Energy ν cm^{-1}**	**S_{ed}(10^{-22} cm^2)**	**A s^{-1}**	**A_T s^{-1}**	**τ_{rad} μs**	**β**	**□a ($10^{-19}cm^2$)**	**S_{ed}(10^{-22} cm^2)**	**A s^{-1}**	**A_T s^{-1}**	**τ_{rad} μs**	**β**	**□a ($10^{-19}cm^2$)**
$^1G_4$	6950	1.48	201	813	1230	0.247	2.5	2.64	359	1431	595	0.2513	4.52
$^3F_4$	9870	1.52	22			0.027	0.14	3.2	45			0.0315	0.3
$^3F_3$	10300	0.1	65			0.079	0.38	0.196	87			0.06	0.5
$^3F_2$	11690	0.125	1			0.001	0.005	0.09	1			0.0001	0.005
$^3H_6$	12340	0.095	71			0.087	0.28	0.489	340			0.238	1.4
$^3H_5$	14520	0.003	3			0.001	0.008	0.009	4			0.003	0.01
$^3H_4$	16840	0.219	450			0.55	0.97	0.276	595			0.4165	1.3

Table 6: Calculated radiative parameters of Dy^{3+} ion in the GDO and DPO crystals Conclusions.

		DGO						DPO					
Transition from $^4F_{9/2}$	**Energy ν cm^{-1}**	**S_{ed}(10^{-22} cm^2)**	**A s^{-1}**	**A_T s^{-1}**	**τ_{rad} µs**	**β**	**□a ($10^{-19}cm^2$)**	**S_{ed}(10^{-22} cm^2)**	**A s^{-1}**	**A_T s^{-1}**	**τ_{rad} µs**	**β**	**□a ($10^{-19}cm^2$)**
$^6F_{1/2}$	7283	0.082	1	1609	622	0.0001	9.7	0.004	1	1358	736	0.0001	9.7
$^6F_{3/2}$	7845	0.1878	1			0.0001	8.4	0.008	1			0.0001	8.4
$^6F_{5/2}$	8649	4.51	7			0.0045	48	1	2			0.002	13.7
$^6F_{7/2}$	10082	0.3	8			0.0046	40	0.3	8			0.005	40
$^6H_{5/2}$	10892	1.509	5			0.003	21	1.2	4			0.004	17
$^6H_{7/2}$	11955	6.7561	29			0.018	10	1.8	8			0.005	3
$^6F_{9/2}$	12039	1.9863	9			0.0053	42	1.92	9			0.006	32
$^6F_{11/2}$	13361	4.5872	26			0.016	75	5.4	33			0.024	95
$^6H_{9/2}$	13390	4.02	23			0.014	66	3.61	21			0.015	61
$^6H_{11/2}$	15269	8.7	74			0.047	16	14.71	126			0.092	28
$^6H_{13/2}$	17670	71.69	930			0.598	154	76.5	1002			0.73	166
$^6H_{15/2}$	21140	19.78	445			0.286	51	6.91	163			0.12	19

Dysprosium Gadolinium oxalate, Dysprosium praseodymium oxalate and gadolinium praseodymium oxalate crystals were grown and characterized using X-ray diffraction and optical absorption spectra. The mixed rare earth crystals are iso structural with individual compounds gadolinium oxalate, praseodymium oxalate and dysprosium oxalate. From the optical absorption spectra radiative properties transition probabilities, radiative life times, branching ratios and absorption cross sections for stimulated emission were determined for $Dy^{3+}$and Pr^{3+} ions using Judd-Ofelt theory. The analysis clearly shows the potentiality of the transitions $^4F_{9/2}\rightarrow{}^6H_{13/2}$ of Dy^{3+} and$^1D_2\rightarrow{}^3H_4$ of Pr^{3+} for giving maximum optical gain.

ACKNOWLEDGEMENT

Vinoy Thomas is thankful to University Grants Commission (UGC, Govt. of India) for financial assistance in the for a research grant.

REFERENCES

1. Lingling P., Tao H., Hui C. and Tiejun Z. (2013) Spectroscopic properties of Gd_2O_3: Dy^{3+} nanocrystals, *J. Rare Earths*, 31(3), 235-240.
2. Chaouki Bensalem, Michel Mortier, Daniel Vivien, Patrick Gredin, Gilles Patriarche, MadjidDiaf (2012) Thermal and Structural Characterization of Transparent Rare-Earth Doped Lead Fluoride Glass-Ceramics, *New J. Glass And Ceramics*, 2, 65 -74
3. Liu Qing, Yan Xiaohong, Chen Yuan, Wang Xiangfu (2013) Upconversion emission of $SrYbF_5$: Er^{3+} nanosheets modified by Tm^{3+} ions, *J. Rare Earths*, 31(11), 1053-1058.
4. Slooff L. H, Van Blaaderen A., Polman A., Hebbink G. A., Klink S. I., Van Veggel F. C. J. M., Reinhoudt D. N. Hofstraat J. W, (2002) Rare-earth doped polymers for planar optical amplifiers, *J. Appl. Phys.*, 91(7), 3955–3980.
5. Zhu Ge, CiZhipeng, Shi Yurong, Wang Yuhua (2013) Synthesis and photoluminescence properties of a red emitting phosphor $NaSr_2$ (NbO_3)5:RE3+ (RE=Sm, Pr) for white LEDs, *J. Rare Earths*, 31(11), 1049-1052.
6. Melcher C. L. and Schweitzer J. S. (1992) Cerium-doped lutetium oxyorthosilicate: a fast, efficient new scintillator, *Nuclear Science,IEEE Transactions*, 39 (4), 502-505.

7. Ramana Reddy M. V., ChGopal Reddy, Narasimha Reddy K., (2007) Thermoluminescence characteristics of Sm3+ doped NaYF4 crystals, *Bull. Mater. Sci.*, 30 (1), 1-3.
8. Soares M. R. N., Nico C., Peres M., Ferreira N., Fernandes A. J. S, Monteiro T., Costa F. M. (2011) Structural and optical properties of europium doped zirconia singlecrystals fibers grown by laser floating zone, *J. Appl. Phys.*, 109, 013516 (1-5).
9. Xu Wu, Shuang-Chen Ruan, Cheng-Xiang Liu, and Li Zhang, (2012) High-stability erbium-doped photonic crystal fiber, *Applied Optics*, 51 (13), 2277-2281.
10. Zhao Y. F., Zhao Y. L., Bai F., Wei X. Y., Zhou Y. S., Shan M.N., Li H. H., Ma R.J., Fu X. T., Du Y. (2010), Fluorescent Property of the Gd3+-Doped Terbium Complexesand Crystal Structure of $[Tb(TPTZ)(H_2O)_6]Cl_3 \cdot 3H_2O$, *J Fluoresc.*, 20(3),763-770.
11. Lihe Zheng, Liangbi Su, Jun XuIn (2013) Modern Aspects Of Bulk Crystal And Thin Films, *Ed. By N KolesnikovIn Tech Publishers.*
12. Lihe Zheng, A. B. Radosławlisiecki C. N., Witoldryba-Romanowski C., Gérardaka B., Juqingdi D., Dongzhen Li D., Xiaodongxu A., Nn, Junxu (2014) Crystal growth and spectroscopic properties of praseodymium and cerium co-doped Y_2SiO_5, *J. Lumin, 145, 547*-552.
13. Dekker R., W. Klunder, D. J. Borreman A., Diemeer M. B. J., Wörhoff K., Driessen A., Stouwdamd, J. W., Van Veggeld F. C. J. M. (2004) Stimulated emission and optical gain in LaF_3 :Nd nanoparticle-dopedpolymer-based waveguides, *Appl. Phys. Lett,*. 85(25),6104-6106
14. Bamzai K. K, NidhiKachroo, Vishal Singh, SeemaVerma (2013) Synthesis, charecterisation and thermal decomposition of pure and Dysprosium doped Ytrrium Phosphate system, *J. Materials*, Doi.Org/10.1155/2013/359514
15. Zhang X., Xing Y, Wang C, Han J., Li J., Ge M., Zeng X., Niu S., (2009) Lanthanide–alkali metals–oxalates coordination polymers: Synthesis and structures of $[Nd(C_2O_4)_{1.5}(H_2O)_3] \cdot 2H_2O$, $Nd(C_2O_4)(CH_3COO)(H_2O)$, $KLn(C_2O_4)_2(H_2O)_4$ (Ln = Y, Tb), *Inorg. Chim. Acta*, 362(4), 1058 - 1064.
16. María Hernández-Molina,Pablo A. Lorenzo-LuisCatalina Ruiz-Pérez (2001) A new coordination mode in oxalate-bridged polymers: molecular and crystal structure of $[Cu_3(C_2O_4)_2(C_2H_8N_2)_4(ClO_4)_2]_n \cdot 2H_2O$, *Cryst Eng. Comm*, 3, 60-63.
17. Que W., Kam C. H., (2002) Up-conversion luminescence of neodymium oxalate nanoparticles/TiO_2/organically modified silane composite thin films derived at low temperature, *Opt. Mater.*, 19(2), 307-312.
18. Korah I., Josep C., Ittyachan M. A. (2007) Growth and characterisation of gadolinium samarium oxalatesingle crystals, *Cryst. Res. Technol.*,42(10), 939-942.
19. John M. V.,. Ittyachen M. A, (1998) Studies on $Ce_2(C_2O_4)_3$. nH_2O crystals grown in hydro silica gel, *Bull. Mater. Sci.*,21 , 387-391.
20. Pragash R., Gijo Jose, Unnikrishnan N. V., C Sudarsanakumar (2011) Energy transfer and thermal studies of Pr3+doped cerium oxalatecrystals, *Bull. Mater. Sci.*, 34(4), 955-961.
21. Vimal G., Kamal P. M., Biju P. R., Cyriac Joseph, Unnikrishnan N. V., Ittyachen M. A., (2013) Synthesis, structural and spectroscopic investigations of nanostructured samariumoxalate crystals, *Spectr. Chim. Acta Part A: Molecular And Biomolecular Spectroscopy* Doi: http://Dx.Doi.Org/10.1016/J.Saa.2013.11.080.
22. Thomas V., Elizebeth A., Thomas H., Jose G., Unnikrishnan N.V., Joseph C., Ittyachen M. A., (2005) Studies on the growth and optical characterization of dysprosium praseodymium oxalate single crystals, *J. Optoelectron. Adv. Mater.*, 7 : 2687-2692.
23. Anit Elizabeth, Vinoy Thomas, Cyriac Joseph, Gijo Jose, M. A. Ittyachen and N. V. Unnikrishnan, (2004) Studies on the growth and optical characterization of dysprosium gadolinium oxalate single crystals, *Cryst. Res. Tech.*, 39,105-110.
24. Maria Czaja, Sabina Body, Joanna Gabrys Pisarska, Zbigniew Mazurak (2009) Applications of Judd–Ofelt theory to praseodymium and samarium ions in phosphate glass, *Opt. Mater.*, 31(12), 1898-1901.

25. Gin Jose, Vinoy Thomas, Gijo Jose,. Paulose P. I,. Unnikrishnan N.V. (2003) Application of a modified Judd–Ofelt theoryto Pr3 doped phosphate glasses and the evaluation of radiative properties, *J. Non-Cryst. Solids*, 319:89-94.
26. Judd B. R, (1962) Optical Absorption Intensities of Rare-Earth Ions, *Phys. Rev.*, 127,750-761.
27. Ofelt G. S, (1962) Intensities of Crystal Spectra of Rare Earth Ions, *J. Chem. Phys.*, 37, 511-520.
28. Carnaal W. T., Hannah Crosswhite, Croswhite H. M. (1965) Energy level structure and transition probabilities in the spectra of the trivalent lanthanides in LaF_3, www.osti.gov/servlets/purl/6417825
29. Goldner P. and Auzel F. (1996) Application of standard and modified Judd–Ofelt theories to a praseodymiumdopedfluorozirconate glass, *J. Appl. Phys.*, 79, 7972-7977.
30. Gupta A. K., Gupta P. K, Jose G. and Unnikrishnan N.V. (2000) Judd-Ofelt intensity parameters and laser analysis of Pr^{3+}.doped phosphate glasses sensitized by Mn^{2+}. Ions, *J. Non. Cryst. Solids.*, 275, 93-106.